Proceedings of the 2003 IAVSD conference, Atsugi, Japan, August 2003.

Analysis of Active Suspension Systems with Hydraulic Actuators

XIAOMING SHEN[1] and HUEI PENG[2]

SUMMARY

Most of the existing active suspension studies assume that an ideal force actuator exists and will carry out the commanded force accurately. In reality, due to the interaction between the hydraulic actuator and suspension system, the lightly damped modes of the plant will generate lightly damped zeros (LDZ) for the servo-loop system, which confines the closed-loop performance to a low frequency range. Converting the active suspension problem formulation into a displacement control problem, as suggested by several recent papers, will not solve this problem. Four candidate remedies to reduce the effect of the LDZ are studied and their potentials and limitations are discussed.

1 INTRODUCTION

Active Suspensions (AS) have been widely studied over the last 20 years, with hundreds of papers published (see [1] for an extensive review). Most of the published results focus on the main-loop designs, i.e., on the computation of the desired control force, as a function of vehicle states and the road disturbance. It is commonly assumed that the commanded force will be produced accurately. Simulations of these main-loop designs were frequently done without considering actuator dynamics, or with highly simplified sub-loop dynamics.

In reality, actuator dynamics can be quite complicated, and interaction between the actuator and the vehicle suspension cannot be ignored. This is especially true for hydraulic actuators, which remain to be one of the most viable choices due to their high power-to-weight ratio, low cost and the fact force can be generated over a prolonged period of time without overheating. However, hydraulic actuators also have several adverse attributes: they are nonlinear and their force generation capabilities are highly coupled to the vehicle body motions [2]. Few experimental verification on AS algorithms have been reported and all are limited to bandwidth of 2-4 Hz [3][4][5].

In other applications such as durability tests, hydraulic actuators have achieved bandwidth of 50Hz or higher successfully. However, in these applications, the closed-loop systems are usually designed to track a displacement signal, rather than a force signal. Some researchers thus speculate that for hydraulic actuators, "force tracking" is harder than "displacement tracking". Several papers have been published to recast the force control problem in AS designs to a displacement control problem [6][7].

But do we really have a fundamental limit in using hydraulic actuators for force control in general? Or is it an application-specific phenomenon? For example, AS systems have to settle for a smaller actuator, while for durability test rigs more powerful actuators and higher supply pressures can be used. AS actuators are commonly placed in parallel with existing spring/damper, while the durability actuators usually are connected in series with

[1] Graduate student, School of Mechanical and Power Energy Engineering, Shanghai Jiao Tong University, China
[2] Corresponding author, Associate Professor, Department of Mechanical Engineering, University of Michigan, Ann Arbor, MI 48109-2125, 734-936-0352, hpeng@umich.edu

vehicle suspensions. Were AS researchers attacking the wrong problem by solving a force tracking problem? If there is a fundamental issue related to force control, can we avoid this fundamental limit by formulating a displacement control problem? Are there other remedies? The main purpose of this paper is to provide answers to these questions.

First, we compare the AS servo-loop control problem with that of durability test rigs. For both AS and durability test rigs, linearized equations are used so that transfer functions and frequency response can be used for the analysis. Since the lightly-damped zeros (LDZ) of the closed-loop system are the main source of performance limit [7], we will solve the closed-loop transfer functions of the two tracking problems (both force and displacement) analytically. The poles and zeros of the closed-loop transfer functions will then be analyzed. By doing so, the fundamental limits imposed by the LDZ will be clearly understood. It is shown that the displacement control problem also has its own pair of LDZ. Furthermore, while the natural frequency of the displacement control LDZ is a little higher, their damping ratio is lower. Therefore, switching to a displacement control problem is not a complete answer.

Subsequently, remedies to reduce the adverse effect of the LDZ are studied. Four candidate approaches are analyzed—new actuator; suspension parameter optimization; add-on mode such as vibration absorbers; and advanced control algorithms. Analysis and simulation results are presented to show the effect of the proposed remedies.

2 MODEL DEVELOPMENT

2.1 Quarter-Car Active Suspension Model with a Hydraulic Actuator

In this section, we will present the model of a quarter-car AS system equipped with a hydraulic actuator. The governing equations of the quarter-car suspension system (Fig. 1) are presented. The two degrees of freedom (DOF) are the vertical motions of the sprung mass (m_s) and unsprung mass (m_{us}), respectively. This 2 DOF system has one external input, $\dot{z}_0$, which is the rate of change of road surface elevation. A force (f) is applied by the active suspension actuator on m_s and m_{us} . The state space model is:

$$\frac{d}{dt}\begin{bmatrix} z_{us}-z_0 \\ \dot{z}_{us} \\ z_s-z_{us} \\ \dot{z}_s \end{bmatrix} = \begin{bmatrix} 0 & 1 & 0 & 0 \\ -\frac{k_{us}}{m_{us}} & -\frac{c_s+c_{us}}{m_{us}} & \frac{k_s}{m_{us}} & \frac{c_s}{m_{us}} \\ 0 & -1 & 0 & 1 \\ 0 & \frac{c_s}{m_s} & -\frac{k_s}{m_s} & -\frac{c_s}{m_s} \end{bmatrix}\begin{bmatrix} z_{us}-z_0 \\ \dot{z}_{us} \\ z_s-z_{us} \\ \dot{z}_s \end{bmatrix} + \begin{bmatrix} 0 \\ -\frac{1}{m_{us}} \\ 0 \\ \frac{1}{m_s} \end{bmatrix} f + \begin{bmatrix} -1 \\ \frac{c_{us}}{m_{us}} \\ 0 \\ 0 \end{bmatrix}\dot{z}_0 \qquad (1)$$

The transfer function from actuator force to suspension stroke is then

$$G_p = \frac{z_s - z_{us}}{f} = \frac{(m_s+m_{us})s^2 + c_{us}s + k_{us}}{m_s m_{us}s^4 + (c_s m_{us} + m_s c_s + m_s c_{us})s^3 + (m_{us}k_s + c_s c_{us} + k_s m_s + m_s k_{us})s^2 + (k_{us}c_s + k_s c_{us})s + k_s k_{us}} \qquad (2)$$

By using standard servo-valve dynamic equations, the hydraulic system is described by:

$$\dot{f} = \frac{\sqrt{2}A_p \cdot \beta \cdot k_{xd}}{V} \cdot x_{sp} \cdot signsqrt(P_s - \text{sign}(x_{sp}) f / A_p) + \frac{2 \cdot A_p^2 \cdot \beta}{V} \cdot (\dot{z}_{us} - \dot{z}_s)$$
$$\dot{x}_{sp} = \frac{1}{\tau}(-x_{sp} + k_{sv} i_{sv}) \qquad (3)$$

where A_p is the piston area, β is the fluid bulk modulus, k_{xd} is the orifice flow coefficient, x_{sp} is the servo valve displacement, $signsqrt(y) \equiv sign(y) \cdot \sqrt{|y|}$, P_s is the supply pressure, V is the cylinder chamber volume, and k_{sv} is the valve gain. Eq.(3) is then linearized, which enables us to do a more in-depth analysis:

$$2C_x x_{sv} + 2A_p(\dot{z}_{us} - \dot{z}_s) = \frac{V}{\beta A_p}\dot{f}$$
$$\tau \dot{x}_{sv} + x_{sv} = K_v i_{sv} \tag{4}$$

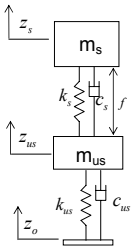

Fig. 1. Quarter-car active suspension model

In Fig. 2, the frequency response of the linear model is plotted against sinusoidal simulation results of the nonlinear system at input magnitude of 7mA (~400N force at 1Hz). It can be seen that Eq.(4) is a good approximation of Eq.(3) under reasonable input magnitude.

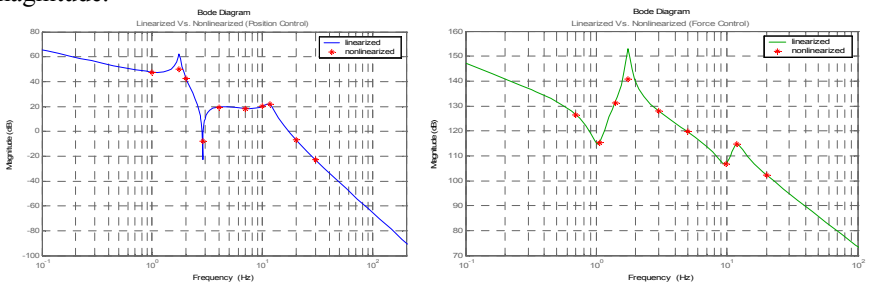

Fig. 2. Validation of the linearization results (suspension stroke and force).

Using the linear approximation of Eq.(4), the dynamics of the overall plant with servo valve current i_{sv} as the control input, has the following form

$$\frac{d}{dt}\begin{bmatrix} z_{us}-z_0 \\ \dot{z}_{us} \\ z_s - z_{us} \\ \dot{z}_s \\ f \\ x_{sv} \end{bmatrix} = \begin{bmatrix} 0 & 1 & 0 & 0 & 0 & 0 \\ -\frac{k_{us}}{m_{us}} & -\frac{c_s + c_{us}}{m_{us}} & \frac{k_s}{m_{us}} & \frac{c_s}{m_{us}} & \frac{-1}{m_{us}} & 0 \\ 0 & -1 & 0 & 1 & 0 & 0 \\ 0 & \frac{c_s}{m_s} & -\frac{k_s}{m_s} & -\frac{c_s}{m_s} & \frac{1}{m_s} & 0 \\ 0 & \frac{2\beta A_p^{\,2}}{V} & 0 & -\frac{2\beta A_p^{\,2}}{V} & 0 & \frac{2c_x \beta A_p}{V} \\ 0 & 0 & 0 & 0 & 0 & -\frac{1}{\tau} \end{bmatrix} \begin{bmatrix} z_{us}-z_0 \\ \dot{z}_{us} \\ z_s - z_{us} \\ \dot{z}_s \\ f \\ x_{sv} \end{bmatrix} + \begin{bmatrix} 0 \\ 0 \\ 0 \\ 0 \\ 0 \\ \frac{k_v}{\tau} \end{bmatrix} i_{sv} + \begin{bmatrix} -1 \\ \frac{c_{us}}{m_{us}} \\ 0 \\ 0 \\ 0 \\ 0 \end{bmatrix} \dot{z}_0 \tag{5}$$

2.2 Active Suspension—Force Control Problem

Given Eq.(5), the transfer function from i_{sv} to f can be obtained:

$$G_{fi} \equiv \frac{f}{i_{sv}} = 2C_x\beta A_p K_v \frac{m_{us}m_s s^4 + (c_{us}m_s + c_s m_s + m_{us}c_s)s^3 + (k_{us}m_s + k_s m_s + c_{us}c_s + m_{us}k_s)s^2 + (k_{us}c_s + c_{us}k_s)s + k_{us}k_s}{D} \quad (6)$$

where the 6th-order denominator polynomial is

$$D = s(s\tau+1)[m_{us}vm_s s^4 + (c_{us}vm_s + c_s vm_s + m_{us}vc_s)s^3 + (2m_{us}\beta A_p^2 + k_s vm_s + c_{us}vc_s + m_{us}k_s v + 2\beta A_p^2 m_s + k_{us}vm_s)s^2 + (2c_{us}\beta A_p^2 + c_{us}k_s v + k_{us}vc_s)s + 2k_{us}\beta A_p^2 + k_{us}k_s v] \quad (7)$$

Similarly, the transfer function from i_{sv} to suspension displacement, $z_s - z_{us}$, is

$$G_{zi} = \frac{z_s - z_{us}}{i_{sv}} = \frac{2C_x\beta A_p K_v[(m_s + m_{us})s^2 + c_{us}s + k_{us}]}{D} \quad (8)$$

Zhang and Alleyne [7] pointed out that the numerator of the transfer function shown in Eq.(6) is the same as the denominator polynomial of the quarter-car suspension plant shown in Eq.(2). This is not a coincidence, and can be explained by formulating a block diagram of the augmented system. Fig. 3 shows a decomposed form of Eq.(5). The "feedback" block $H(s)$ does not represent a feedback control action. Rather, it is an inherent coupling between suspension motion and hydraulic force generation. From Fig. 3 and Eqs.(4)(5), it can be seen that $G_p(s)$ is the suspension dynamics shown in Eq.(2). The force generation dynamics, Eq.(4), can be written as $f = G_a i_{sv} - G_a H y$, where $G_a = \frac{2\beta A_p C_x K_v}{V}\frac{1}{\tau s + 1}$ and $H = \frac{A_p s(\tau s + 1)}{C_x K_v}$.

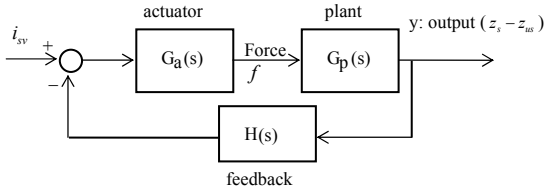

Fig. 3. Block diagram of the suspension displacement sub-loop.

When an engineer is designing the servo-loop control algorithm to ensure proper force generation from the hydraulic actuator, he/she is facing a dynamic system shown in Fig. 4. Again, the two blocks shown in the "feedback loop" were not from a feedback control algorithm, but rather is a physical feedback the control designer has to deal with.

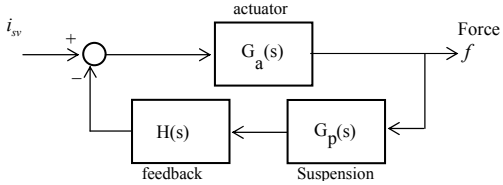

Fig. 4. Block diagram of the actuator force sub-loop.

Given Fig. 4, the "plant' to be controlled is:

$$G_{fi} = \frac{f}{i_{sv}} = \frac{G_a}{1 + G_a G_p H} \tag{9}$$

Obviously, the poles of the active suspension plant (G_p) become zeros of G_{fi} . From Eq.(6), we can see that this is indeed the case. Why is this a concern? Because the active suspension plant (shown in Eq.(2)) includes two under-damped modes (at around 1Hz and 10Hz). The small damping of the tire mode (~0.01-0.03) and the suspension mode (~0.02-0.3?)implies that the plant of the force servo loop (G_{fi} shown in Eq.(9)) will have a pair of under-damped zeros at around 1Hz. For feedback-only control algorithms, the under-damped zeros will remain to be zeros of the closed-loop system. Therefore, the closed-loop bandwidth will be limited by this pair of lightly damped zeros.

What if we use other control configurations? After all, nonlinear algorithms based on the cancellation of suspension-actuator interactions have been proposed and a somewhat higher closed-loop tracking performance has been reported [8][9]. Let's refrain from analyzing specific control algorithms, and instead examine this problem from a more fundamental viewpoint. Assuming that we know little about the servo-loop control algorithm, except that it is "doing a good job". Based on the "perfect control" analysis [10][11], the "well-behaved" control algorithm will generate an inverse of the plant. In other words, a pair of lightly damped zeros (LDZ) demand much larger control actions at their resonant frequency for acceptable control performance. This is theoretically possible but usually difficult to realize in practice.

From the above analysis, and the fact that hydraulic actuators have been used in displacement-tracking applications such as durability test rigs up to 50-80 Hz, it is tempting to claim that reformulating the AS sub-loop problem (from force control) into a displacement tracking problem will be the answer. As mentioned in Section 1, several prior publications based on this belief were published [6][7][12], and two ways to recast the AS servo-loop into displacement tracking problems were proposed.

2.3 Active Suspension—Displacement Control Problem

In this section, by following the same procedure shown in Section 2.2, we examine whether the performance limitation imposed by the LDZ can be removed in the displacement control problem. The system configuration is still the one shown in Fig. 1, and the control problem is to manipulate the servo-valve current so that a desired suspension displacement is followed. The plant of this control problem is shown in Fig. 3. Its transfer function is:

$$G_{zi} = \frac{z_s - z_{us}}{i_{sv}} = \frac{G_a G_p}{1 + G_a G_p H} \tag{10}$$

Obviously, the zeros of the suspension plant (G_p) are also zeros of G_{zi} . This fact is confirmed by examining Eqs. (2) and (8). From Eq.(8), it is obvious that the small tire damping creates a pair of LDZ for G_{zi} . The resonant frequency of these zeros is at around 3Hz (vs. 1Hz for the force loop). In other words, the limitation for tracking performance (as analyzed by the "perfect control" analysis) is somewhat relieved, but not by much. In fact, while the resonant frequency of the LDZ of G_{zi} is higher, their damping ratio is

much lower. This fundamental performance limit arises from low tire damping, and thus design changes such as using a larger and more powerful hydraulic actuator or a faster servo valve will not help.

3. DURABILITY TEST RIG

Before we discuss possible remedies to address the negative impact imposed by the LDZ, let's first examine why this has not been a problem for other hydraulic applications such as durability test rigs. In Fig. 5, a simplified one degree-of-freedom durability test rig is shown. The mass-spring-damper system shown on the top represents the dominate mode of the tested system. The weight of the ground plate plus the tire(s) is denoted as m_{us}. It is straightforward to find the following two transfer functions

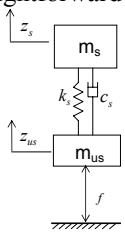

Fig. 5. Durability Test Rig model.

$$G_{p2} = \frac{z_{us}}{f} = \frac{m_s s^2 + c_s s + k_s}{s^2[m_s m_{us} s^2 + (c_s m_{us} + m_s c_s)s + m_s k_s + m_{us} k_s]} \tag{11}$$

$$G_{zi2} = \frac{z_{us}}{i_{sv}} = \frac{2C_x \beta A_p K_v (m_s s^2 + c_s s + k_s)}{D'} \tag{12}$$

where $D' = s(s\tau + 1)[m_{us} v m_s s^4 + (c_s v m_s + m_{us} v c_s)s^3 + (k_s v m_s + m_{us} k_s v + 2\beta A_p{}^2 m_s)s^2 + 2c_s \beta A_p{}^2 s + 2k_s \beta A_p{}^2]$.

The zeros of the plant shown in Eq.(11) are again zeros of the displacement servo-loop, shown in Eq.(12). Since the damping ratio of these zeros is higher than those of Eq.(8) (~0.3 vs. ~0.02), the imposed limitation on tracking performance is much easier to deal with.

4. POSSIBLE REMEDIES

In this section, we will discuss possible remedies (design changes) to address the adverse effects of LDZ on AS systems. These changes aim to eliminate the LDZ, or to increase their damping ratio. Both force and displacement problems are discussed. Here we are not trying to distinguish whether the target application is for narrow band (< 3Hz) or wide band (>10Hz). Rather, we will focus on the influence of the working principle of a force-producing actuator on the servo-loop performance. It should be pointed out that while LDZ problem can be addressed by pole/zero cancellation, this method is not considered because of its poor robustness in real implementations.

4.1 Alternative actuator system

The results presented in this paper so far assume a hydraulic actuator is used. As pointed out earlier, the LDZ arise from the suspension plant (shown in Eq.(2)). Therefore,

modification of the hydraulic actuator system (higher supply pressure, larger cylinders, faster servo valves) will not be effective.

When an electromagnetic, a pneumatic or a piezoelectric actuator is used, a "physical feedback" (the H(s) block in Fig. 3) still exists, although in different forms. For example, in the voltage control mode, a DC motor will have back electromotive force, and for pneumatic actuators, volume/pressure coupling effect exists. The fact such physical feedbacks exist implies that LDZ are present and pose a problem for the control design.

When an actuator without physical feedback is used, the servo-loop is no longer in the form shown in Fig. 3, and the analysis results discussed in the previous two sections need to be modified. An example of force actuators that do not exhibit a physical feedback path is electromagnetic motors running under current drive mode. Since the motor current is supplied regardless of the motor speed, the servo-loop control system is independent of the suspension plant, which is depicted in Fig. 6. Obviously, since $G_p(s)$ is outside of the servo-loop, the LDZ no longer exists for the force sub-loop. For the displacement tracking problem, however, LDZ still exist because $G_p(s)$ is inside the servo-loop.

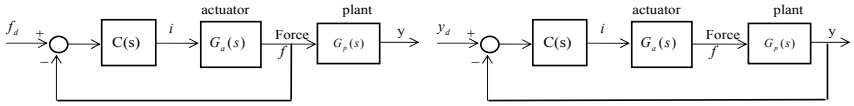

Fig. 6. Block diagrams of the force sub-loop and displacement sub-loop for a current-mode drive electric actuator.

4.2 Effect of modified suspension parameters

In this sub-section, we will examine the effect of modified suspension parameters on the characteristics of the LDZ. In particular, we will focus on their effect on the damping ratio of the LDZ. We assume that the sprung mass is given and cannot be assigned. The nominal values of the suspension parameters are shown in Table 1.

Table 1. Nominal values of the suspension parameters.

Parameter	Meaning	Value	Parameter	Meaning	Value
m_s	Sprung mass	$253kg$	c_{us0}	Tire damping	$10N/m/\sec$
m_{us0}	Unsprung mass	$26kg$	k_{s0}	Suspension stiffness	$12000N/m$
c_{s0}	Suspension damping	$348.5N/m/\sec$	k_{us0}	Tire stiffness	$90000N/m$

4.2.1 Displacement control problem

Only three parameters will influence the LDZ: m_{us}, c_{us} and k_{us} (see Eq.(2)). Apparently, the most important parameter is the tire damping c_{us}. Increasing c_{us} will increase the damping ratio of the LDZ. However, since this will also increase rolling resistance, it is quite obvious little room is left for the designer.

4.2.2 Force control problem

Five parameters will influence the LDZ (numerator of Eq.(6)): c_s, k_s, m_{us}, c_{us} and k_{us}. Note that there are two pairs of LDZ. We varied all five parameters within a range of

their nominal values, depending on our judgment of what could be achieved in practice. It was found that perturbing suspension damping (c_s) or suspension stiffness (k_s) are most effective. The effect of c_s and k_s on the smaller of the two damping ratios is shown in Fig. 7. The effect of c_s is not monotonic because the faster mode becomes less damped than the slower mode at high frequency. We can increase LDZ damping by either increasing c_s or decreasing k_s. For example, if we increase c_s by a factor of 7, the damping ratio will become 0.6, high enough that the zeros no longer pose a problem for the control design. Smaller improvement can be achieved by reducing k_s. Changing these two parameters needs to be done carefully by weighing against their adverse effect—reduced actuator energy efficiency and increased rattle space, respectively.

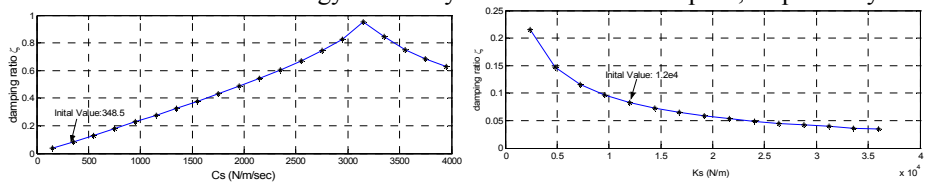

Fig. 7. Effect of perturbing suspension damping and stiffness on damping of LDZ.

To study the effect of c_s, an AS efficiency is defined as $\eta = 1 - E_{wasted} / E_{total}$, where the total input energy E_{total} and the energy absorbed by c_s, E_{wasted} are

$$E_{total}(t) = \int_0^t f \cdot (\dot{z}_s - \dot{z}_{us}) d\tau, \quad f \cdot (\dot{z}_s - \dot{z}_{us}) > 0$$
$$E_{wasted} = \int_0^t \min\{f \cdot (\dot{z}_s - \dot{z}_{us}),\ c_s (\dot{z}_s - \dot{z}_{us})^2\} d\tau, \quad f \cdot (\dot{z}_s - \dot{z}_{us}) > 0 \tag{13}$$

The force f used is commanded from a main-loop LQ algorithm, where the control gains are re-computed for each perturbed c_s. The relationship between c_s and η is shown in Fig. 8(a). Increasing c_s results in an almost monotonic reduction in η. If we increase c_s by a factor of 7, η will reduce from 60% to 20%. This may be unacceptable because power consumption and cooling requirement. The most obvious adverse effect of a softer suspension (smaller k_s) is increased rattle space (shown in Fig. 8(b)) and body leaning during cornering. In other words, in practice there is limited room for a control engineer to improve the damping of LDZ by reducing k_s.

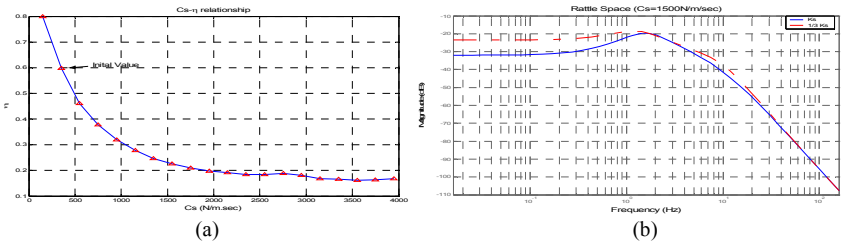

(a) (b)

Fig. 8. Effect of modified suspension damping and stiffness.

4.3 Vibration absorber

A vibration absorber (VA) refers to a single degree of freedom mass-spring oscillator with low (no) damping. The basic idea for using a vibration absorber is that the mode associated with the additional "energy storage buffer" creates a pair of zeros at the designed frequency. Here we introduce a lightly-damped vibration absorber attached to the unsprung mass (see Fig. 9). The suspension dynamics become

$$G_p = \frac{z_s - z_{us}}{f} = \frac{m_a(m_{us}+m_s)s^4 + (m_a c_{us} + m_{us}c_a + c_a m_a + c_a m_s)s^3}{d} + \frac{(k_a m_a + k_a m_s + m_{us}k_a + k_{us}m_a + c_{us}c_a)s^2 + (c_{us}k_a + k_{us}c_a)s + k_{us}k_a}{d}$$

$$\underset{m_a << m_s}{\approx} \frac{(m_a s^2 + c_a s + k_a)[(m_{us}+m_s)s^2 + c_{us}s + k_{us}]}{d} \qquad (14)$$

where, by using the facts $m_a << m_s$, $c_a << c_s$ and $k_a << k_{us}$

$$d \approx (k_a + c_a s + m_a s^2)(m_s s^2 + c_s s + k_s)(m_{us}s^2 + c_{us}s + k_{us}) + (k_a + c_a s + m_a s^2)(c_s m_s s^3 + k_s m_s s^2)$$
$$= (k_a + c_a s + m_a s^2)[(m_s s^2 + c_s s + k_s)(m_{us}s^2 + c_{us}s + k_{us}) + k_s m_s s^2 + c_s m_s s^3] \qquad (15)$$

Notice that both the numerator and denominator approximately contain a vibration mode $(k_a + c_a s + m_a s^2)$, which results in a near-pole-zero cancellation for G_{fi} and G_{zi}. Therefore, the effect of VA is localized. Simulations in Fig. 10 show that the vibration absorber is not effective for the force control loop. For the displacement control problem, the vibration absorber can reduce the adverse effect of LDZ by almost 30dB (at 3Hz), by properly tuning the VA damping c_a.

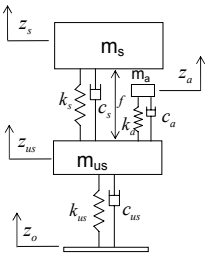

Fig. 9. Quarter-car suspension model with vibration absorber.

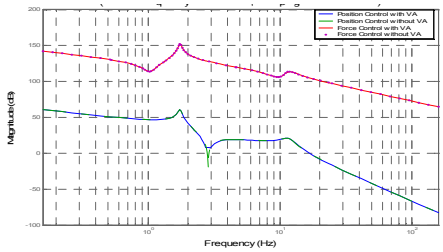

Fig. 10. Frequency response of vibration absorber.

4.4 Advanced control algorithms

By employing advanced control strategies, we can cancel the physical feedback introduced by the hydraulic actuator (or other actuators). Therefore, the effect of this

remedy is similar to introducing a non-feedback actuator discussed in Section 4.1. We can even state that the current-mode motor control concept is a special case of the advanced control based algorithm. Inside the current-mode drive is a feedback law that cancels the back electromotive force. This "using feedback control to cancel physical feedback" idea can be applied to other actuator systems. For hydraulic actuators, we expect this to be much harder to achieve because the large bulk modulus of hydraulic fluids represents a rigid coupling. Fast sensing of hydraulic pressure and subsequent manipulation of pumps/valves to react to pressure increase/drop is harder compared with current-mode motor drive. Therefore, this remedy may not work well with hydraulic actuators. No matter which actuator system is used, the servo-loop control algorithm and hardware need to be designed to work with the surge in control signal magnitude at the resonant frequency of LDZ.

5. CONCLUSION

The inherited challenge and possible remedies of the servo-loop control design for active suspension systems are presented. It is shown that for both force servo-loop and displacement servo-loop, we have lightly damped zeros (LDZ) in the "plant", which impose performance limit in practical implementations. It was found that recasting the active suspension servo-loop into a displacement control problem does not provide significant benefits. Four possible remedies were studied—different actuation systems, modified suspension parameters, vibration absorbers, and advanced control algorithms. It was found these remedies can either completely eliminate the LDZ, or moderately increase their damping ratio so that the imposed performance limit is reduced.

REFERENCES

1. Hrovat, D., (1997) "Survey of Advanced Suspension Developments and Related Optimal Control Applications," Automatica, v 33 n 10, pp.1781-1817.
2. Alleyne, A., Liu, R., (1999) "On the limitations of force tracking control for hydraulic servo systems," Journal of Dynamic Systems, Measurement and Control, Trans. of the ASME, Vol. 121, n. 2, 1999, pp. 184-190.
3. Alleyne, A., Hedrick, J.K., (1995) "Nonlinear Adaptive Control of Active Suspension," IEEE Trans. on Control Systems Technology, Vol. 3, n. 1, March, pp. 94-101.
4. Goran, M. B., Bachrach, B. I., Smith, R. E., (1992) "The Design and Development of a Broad Bandwidth Active Suspension Concept Car," ImechE 1992, pp. 231-252.
5. Rajamani, R., Hedrick, J.K., (1994) "Performance of Active Automotive Suspensions with Hydraulic Actuators: Theory and Experiment," Proc. of the American Control Conference, June 1994, pp. 1214-1218.
6. Peng, H., Strathearn, R., Ulsoy, A.G., "A Novel Active Suspension Design Technique--Simulation and Experimental Results," Proceedings of the 1997 American Control Conference, Albuquerque, New Mexico, June 4-6, 1997.
7. Zhang, Y., Alleyne, A., "A Practical and Effective Approach to Active Suspension Control," Proceedings of the 6th International Symposium on Advanced Vehicle Control, Hiroshima, Japan, September 2002.
8. Chantranuwathana, S. and Peng, H., "Practical Adaptive Robust controller for Active Suspensions," Proceedings of the 2000 ASME International Congress and Exposition, Orlando, Florida.
9. Chantranuwathana, S., *Adaptive Robust Force Control For Vehicle Active Suspensions*, Ph.D. Dissertation, University of Michigan, 2001.
10. Skogestad, S. and Postlethwaite, I., Multivariable Feedback Control—Analysis and Design, Wiley, 1996.
11. Morari, M., "Design of Resilient Processing Plants—III, A General Framework for the Assessment of Dynamic Resilience," Chemical Engineering Science, Vol.38, No.11, pp.1881-1891, 1983.
12. Zhang, Yisheng, Alleyne, A., "A New Approach to Half-Car Active Suspension Control," Proceedings of the 2003 American Control Conference, Denver, Colorado.